



ANM analysis of a wrinkled elastic thin membrane

Siham Khalil^a, Youssef Belaasilia^a, Abdellah Hamdaoui^a, Bouazza Braikat^{a,*},
 Mohammad Jamal^a, Nouredine Damil^a, Zitouni Azari^b

^a Laboratoire d'Ingénierie et Matériaux (LIMAT), Faculté des Sciences Ben M'Sik, Hassan II University of Casablanca, BP 7955, Sidi Othman, Casablanca, Morocco

^b Laboratoire d'Étude des Microstructures et de Mécanique des Matériaux, LEM3, CNRS, UMR 7239, École Nationale d'Ingénieurs de Metz (ENIM), Université de Lorraine, 1, route d'Ars-Laquenexy, 57078 Metz, France



ARTICLE INFO

Article history:

Received 5 August 2019

Accepted after revision 3 October 2019

Available online 21 October 2019

Keywords:

Wrinkles disappearance
 Asymptotic Numerical Method
 Membrane effect
 Föppl–von Kármán model

ABSTRACT

In this work, we have investigated numerically the disappearance of wrinkles from a tensed membrane by the Asymptotic Numerical Method (ANM) using the finite-element DKT18. The ANM is a path-following technique that has been used to solve bifurcation problems. We show numerically the influence of the terms corresponding to the membrane displacement gradient in the Föppl–von Kármán (FvK) theory on the bifurcation curves in the case of a stretched elastic membrane. We will also study numerically, by using the ANM algorithm, the influence of the thickness and of the aspect ratio on the re-stabilization of a rectangular elastic membrane during stretching. The results obtained by our model are compared with those obtained using the industrial code ABAQUS.

© 2019 Académie des sciences. Published by Elsevier Masson SAS. All rights reserved.

1. Introduction

Thin structures are often subjected to compressive or tensile stresses. When these stresses exceed a critical value, a geometric instability phenomenon occurs, which results in an out-of-plane deformation of the structure. This instability appears in inflatable structures such as life jackets [1] or on metal sheets at the exit of a rolling mill [2]. In the case of plates and shells, the instability usually occurs at the global scale; it is global buckling. In membranes, instability occurs at the local level; it is local buckling or wrinkling. The study of thin structures buckling generally leads to the resolution of eigenvalue problems. A wrinkling membrane is a more complex phenomenon, because it involves two levels of scales: the local and the global scales. The study of these phenomena requires then the resolution of nonlinear multi-scale problems. The methods of solving problems of wrinkling membranes are various and varied.

During the last decade, theoretical, numerical, and experimental studies have been devoted to stability analyzes to determine the critical conditions of instability and the corresponding modes [3–7]. In the work [8], the authors have modified the Föppl–von Kármán model, in the simplest manner possible, accounting for the finite mid-plane deformation of the highly stretched state. The obtained problem is solved by the Euler–Newton arc-length continuation [9] using a so-called conformal finite-element discretization. The buckling due to global tension of a rectangular thin membrane in the absence of any geometric discontinuity is studied numerically and analytically by Friedl et al. [10]. In [11], further authors have extended the constitutive models; the material is considered to be hyper-elastic, such as in the neo-Hookean (nHk) model

* Corresponding author.

E-mail address: b.braikat@gmail.com (B. Braikat).

and the Mooney–Rivlin (MR) model. In reference [12], the authors have presented a simple pseudo-elastic model, capturing the stress softening and residual strain, during the stretching of a thin membrane. In [13], the authors explore the wrinkling and re-stabilization behavior, both analytically and numerically, based respectively on Koiter stability theory and the commercial finite-element package Abaqus. The authors of reference [14] have developed a modeling and resolution framework to solve the complex instability problem with highly geometric and material nonlinearities of stretched rectangular hyper-elastic membranes. This numerical resolution framework is based on a path-following continuation technique combining the ANM with a discretization by a spectral method. The ANM is an algorithm for numerical resolution of nonlinear problems depending on a scalar parameter [15,16]. The solutions are thus determined branch by branch, each branch is determined analytically using a Taylor vectorial series representation, truncated at a high order from an initial solution point. The terms of the vectorial series are determined numerically by inverting only one stiffness matrix for each branch. This method has proved its effectiveness in the study of bifurcated branches in post-buckling elastic shells [17–19]. The ANM algorithm coupled with finite elements will be used, in this paper, for the first time to study the influence of three bifurcation parameters (the thickness, the aspect ratio and the load parameter) on the wrinkling disappearance of stretched elastic membrane.

In this paper, we studied two types of deformations: the first one corresponds to the model of Föppl–von Kármán, and the second one takes into account products of the gradient of membrane displacements. The two obtained problems are solved by both the Asymptotic Numerical Method (ANM) using the finite-element DKT18 [20] and the industrial Abaqus code using the finite-element S8R. A comparative study between the two obtained results has been done. We have also demonstrated that the use of this algorithm has greatly reduced the computational time comparing to the Abaqus code and made the continuation easier. Indeed, the solution was obtained using a single combination of the parameters of the ANM algorithm, the truncation order and the tolerance parameter, from the starting point.

This article is organized as follows. In Section 2, a modified Föppl–von Kármán plate theory is presented in detail. Section 3 is devoted in detail to the resolution strategy by the ANM algorithm. Next, in Section 4, a benchmark example related to wrinkling disappearance analysis is analyzed by this ANM algorithm to assess its efficiency and reliability.

2. Modified Föppl–von Kármán plate theory

In our study, we assume that the 3D structure is a thin membrane. For this purpose, we use the kinematics of Love–Kirchhoff. The 3D displacement field $(U(x, y, z), V(x, y, z), W(x, y, z))$ is defined by those of the average surface $(u(x, y), v(x, y), w(x, y))$ in the following form:

$$\begin{cases} U(x, y, z) = u(x, y) + z\beta_x(x, y) \\ V(x, y, z) = v(x, y) + z\beta_y(x, y) \\ W(x, y, z) = w(x, y) \end{cases} \quad (1)$$

where $\beta_x(x, y) = -w_{,x}(x, y)$ and $\beta_y(x, y) = -w_{,y}(x, y)$ are the rotations around the x - and y -axes, respectively. According to the nonlinear membrane theory, one can write the expression of the generalized Green–Lagrange strain vector $\{\gamma\} = {}^t < \gamma_{xx}, \gamma_{yy}, 2\gamma_{xy}, k_{xx}, k_{yy}, 2k_{xy} >$ as a function of displacements in the following form [8,11]:

$$\{\gamma\} = \{\gamma^l\} + \{\gamma^{nl}\} \quad (2)$$

where $\{\gamma^l\}$ is the linear strain vector and $\{\gamma^{nl}\}$ is the nonlinear strain vector represented by their components in the following form:

$$\{\gamma^l\} = \begin{Bmatrix} u_{,x} \\ v_{,y} \\ u_{,y} + v_{,x} \\ \beta_{x,x} \\ \beta_{y,y} \\ \beta_{x,y} + \beta_{y,x} \end{Bmatrix} ; \quad \{\gamma^{nl}\} = \begin{Bmatrix} \frac{1}{2}(u_{,x}^2 + v_{,x}^2 + w_{,x}^2) \\ \frac{1}{2}(u_{,y}^2 + v_{,y}^2 + w_{,y}^2) \\ u_{,x}u_{,y} + v_{,x}v_{,y} + w_{,x}w_{,y} \\ 0 \\ 0 \\ 0 \end{Bmatrix} \quad (3)$$

where $(.)_{,j}$ is the derivative with respect to the j -th spatial component. When we neglect the terms of order 2 of $u_{,x}$, $u_{,y}$, $v_{,x}$ and $v_{,y}$, we obtain the deformations of Föppl–von Kármán plates.

To write Eq. (2) in a matrix form, one introduces the gradient vector $\{\theta\}$ given by:

$$\{\theta\} = {}^t < u_{,x}, u_{,y}, v_{,x}, v_{,y}, w_{,x}, w_{,y}, \beta_{x,x}, \beta_{x,y}, \beta_{y,x}, \beta_{y,y} > \quad (4)$$

From Eq. (4), the generalized Green–Lagrange strain vector $\{\gamma\}$ can be written in the following form:

$$\{\gamma\} = ([H] + \frac{1}{2}[A(\{\theta\})])\{\theta\} \quad (5)$$

where the matrices $[H]$ and $[A(\{\theta\})]$ are given by:

$$[H] = \begin{bmatrix} 1 & 0 & 0 & 0 & 0 & 0 & 0 & 0 & 0 & 0 \\ 0 & 0 & 0 & 1 & 0 & 0 & 0 & 0 & 0 & 0 \\ 0 & 1 & 1 & 0 & 0 & 0 & 0 & 0 & 0 & 0 \\ 0 & 0 & 0 & 0 & 0 & 0 & 1 & 0 & 0 & 0 \\ 0 & 0 & 0 & 0 & 0 & 0 & 0 & 0 & 0 & 1 \\ 0 & 0 & 0 & 0 & 0 & 0 & 0 & 1 & 1 & 0 \end{bmatrix}; [A(\{\theta\})] = \begin{bmatrix} u_{,x} & 0 & v_{,x} & 0 & w_{,x} & 0 & 0 & 0 & 0 & 0 \\ 0 & u_{,y} & 0 & v_{,y} & 0 & w_{,y} & 0 & 0 & 0 & 0 \\ u_{,y} & u_{,x} & v_{,y} & v_{,x} & w_{,y} & w_{,x} & 0 & 0 & 0 & 0 \\ 0 & 0 & 0 & 0 & 0 & 0 & 0 & 0 & 0 & 0 \\ 0 & 0 & 0 & 0 & 0 & 0 & 0 & 0 & 0 & 0 \\ 0 & 0 & 0 & 0 & 0 & 0 & 0 & 0 & 0 & 0 \end{bmatrix} \quad (6)$$

In the case of the Föppl–von Kármán deformation, the matrix $[A(\{\theta\})]$ is classically written as:

$$[A(\{\theta\})] = \begin{bmatrix} 0 & 0 & 0 & 0 & w_{,x} & 0 & 0 & 0 & 0 & 0 \\ 0 & 0 & 0 & 0 & 0 & w_{,y} & 0 & 0 & 0 & 0 \\ 0 & 0 & 0 & 0 & w_{,y} & w_{,x} & 0 & 0 & 0 & 0 \\ 0 & 0 & 0 & 0 & 0 & 0 & 0 & 0 & 0 & 0 \\ 0 & 0 & 0 & 0 & 0 & 0 & 0 & 0 & 0 & 0 \\ 0 & 0 & 0 & 0 & 0 & 0 & 0 & 0 & 0 & 0 \end{bmatrix} \quad (7)$$

The constitutive law for an isotropic, elastic, homogeneous structure on the average surface ω is defined by the following relation:

$$\{S\} = [D]\{\gamma\} \quad (8)$$

where $\{S\} = {}^t \langle N_{xx}, N_{yy}, N_{xy}, M_{xx}, M_{yy}, M_{xy} \rangle$ is the generalized stress vector and $[D]$ is the stiffness matrix, which depends on the Young modulus E , on the Poisson’s ratio ν , and on the thickness h , and is given by:

$$[D] = \begin{bmatrix} C_m & \nu C_m & 0 & 0 & 0 & 0 \\ \nu C_m & C_m & 0 & 0 & 0 & 0 \\ 0 & 0 & \frac{(1-\nu)}{2} C_m & 0 & 0 & 0 \\ 0 & 0 & 0 & C_b & \nu C_b & 0 \\ 0 & 0 & 0 & \nu C_b & C_b & 0 \\ 0 & 0 & 0 & 0 & 0 & \frac{(1-\nu)}{2} C_b \end{bmatrix} \quad (9)$$

where $C_m = \frac{Eh}{1-\nu^2}$ and $C_b = \frac{Eh^3}{12(1-\nu^2)}$ represent respectively the membrane and bending rigidity coefficients.

The complete problem representing the equilibrium of this structure modeled by its average surface and subjected to a $\lambda\{f\}$ is written in the following form:

$$\begin{cases} \int_{\omega} \langle \delta\theta \rangle {}^t([H] + [A(\{\theta\})])\{S\} d\omega = \lambda P_{\text{ext}}(\delta u) \\ \{S\} = [D]\{\gamma\} \\ \{\gamma\} = ([H] + \frac{1}{2}[A(\{\theta\})])\{\theta\} \end{cases} \quad (10)$$

where $P_{\text{ext}}(\delta u)$ is the work of external efforts and λ is a scalar loading parameter. The resolution of the problem (10) completed by the boundary conditions is done by the Asymptotic Numerical Method (ANM), which will be the object of the following section.

3. Numerical simulation by the Asymptotic Numerical Method (ANM)

There are several numerical methods for solving the nonlinear problem (10). In this work, for this kind of problems, we adopt for the first time the Asymptotic Numerical Method coupled with the finite-element method [15,16]. This method is based on three steps; a Taylor series representation, a spatial discretization, and a continuation method, which enabled us to calculate the solution to the nonlinear problem as a succession of branches. Each branch is obtained by inverting only a single tangent stiffness matrix.

3.1. Taylor series representation

The purpose of this step is to transform the nonlinear problem (10) into a sequence of linear problems having the same tangent operator by developing the unknowns $(u, \lambda, \{\theta\}, \{\gamma\}, \{S\})$ of the nonlinear problem with respect to a path parameter a in the neighborhood of a known solution $(u^j, \lambda^j, \{\theta^j\}, \{\gamma^j\}, \{S^j\})$, as follows:

$$\begin{cases} u(a) = u^j + \sum_{k=1}^{k=p} u_k a^k \\ \lambda(a) = \lambda^j + \sum_{k=1}^{k=p} \lambda_k a^k \\ \{\theta\}(a) = \{\theta^j\} + \sum_{k=1}^{k=p} \{\theta_k\} a^k \\ \{\gamma\}(a) = \{\gamma^j\} + \sum_{k=1}^{k=p} \{\gamma_k\} a^k \\ \{S\}(a) = \{S^j\} + \sum_{k=1}^{k=p} \{S_k\} a^k \end{cases} ; a \in [0, a_{\max}] \tag{11}$$

where $u_k, \lambda_k, \{\theta_k\}, \{\gamma_k\}$ and $\{S_k\}$ are terms of Taylor series at each order k , p is the truncation order and a_{\max} is the validity range. The parameter a is defined by the additional equation; in this paper, we choose an arc length relation of the form $a = (u(a) - u^j)u_1 + (\lambda(a) - \lambda^j)\lambda_1$. Taking into account the formula (11), the nonlinear problem (10) is transformed into a succession of linear problems given by:

$$\begin{aligned} \text{Order } k = 1 & ; \begin{cases} \int_{\omega} \langle \delta\theta \rangle ({}^t([H] + [A(\{\theta^j\})])\{S_1\} + [\hat{S}]\{\theta_1\}) d\omega = \lambda_1 P_{\text{ext}}(\delta u) \\ \{S_1\} = [D]\{\gamma_1\} \\ \{\gamma_1\} = ([H] + [A(\{\theta^j\})])\{\theta_1\} \end{cases} \\ \text{Order } 2 \leq k \leq p & ; \begin{cases} \int_{\omega} \langle \delta\theta \rangle ({}^t([H] + [A(\{\theta^j\})])\{S_k\} + [\hat{S}]\{\theta_k\}) d\omega = \lambda_k P_{\text{ext}}(\delta u) + f_k^{\text{nl}} \\ \{S_k\} = [D]\{\gamma_k\} \\ \{\gamma_k\} = ([H] + [A(\{\theta^j\})])\{\theta_k\} + \{\gamma_k^{\text{nl}}\} \end{cases} \end{aligned} \tag{12}$$

where f_k^{nl} and $\{\gamma_k^{\text{nl}}\}$ are the right-hand sides, which depend on the previous orders given by:

$$\begin{cases} f_k^{\text{nl}} = - \int_{\omega} \langle \delta\theta \rangle (\sum_{r=1}^{k-1} {}^t[A\{\theta_r\}]\{S_{k-r}\}) d\omega \\ \{\gamma_k^{\text{nl}}\} = \frac{1}{2} \sum_{r=1}^{k-1} [A(\theta_r)]\{\theta_{k-r}\} \end{cases} \tag{13}$$

The quantity $[\hat{S}]$ is a matrix that depends on the membrane efforts N_{xx}, N_{yy} , and N_{xy} .

3.2. Spatial discretization

The domain ω occupied by the mid-surface of the studied structure is discretized into finite elements of type DKT18 [20]. This finite element has three nodes, which each have six degrees of freedom: three displacements and three rotations. In each finite element, the displacement vector $\{u^e\}$ and the gradient vector $\{\theta^e\}$ at a point of this element is approximated by the following expressions:

$$\begin{cases} \{u^e\} = [N]\{q^e\} \\ \{\theta^e\} = [G]\{q^e\} \end{cases} \tag{14}$$

where $[N]$ is the matrix of shape functions, $[G]$ is the matrix of shape functions gradient, and $\{q^e\}$ is the corresponding elementary displacements vector. Taking into account this approximation and the assembly technique, the problem (12) becomes:

$$\begin{aligned} \text{Order } k = 1 & ; \begin{cases} [K_T]\{Q_1\} = \lambda_1 \{F\} \\ \langle Q_1 \rangle \{Q_1\} + \lambda_1^2 = 1 \end{cases} \\ \text{Order } 2 \leq k \leq p & ; \begin{cases} [K_T]\{Q_k\} = \lambda_k \{F\} + \{F_k^{\text{nl}}\} \\ \langle Q_1 \rangle \{Q_k\} + \lambda_1 \lambda_k = 0 \end{cases} \end{aligned} \tag{15}$$

where $[K_T]$ is the tangent stiffness matrix, $\{F\}$ is the vector of external forces, $\{F_k^{\text{nl}}\}$ is a right-hand-side term that depends on the previous orders and $\{Q_k\}$ is a global unknown displacement vector.

3.3. Continuation method

The whole solution to the nonlinear problem is obtained step-by-step using a continuation path-following method [21]. It allows us to compute a succession of different branches. The evaluation of the solution at the end of each step becomes the new starting point of the next step. Each step-length is given in an optimum way by:

$$a_{\max} = \left(\varepsilon \frac{\| \{Q_1\} \|}{\| \{Q_p\} \|} \right)^{\frac{1}{p-1}} \tag{16}$$

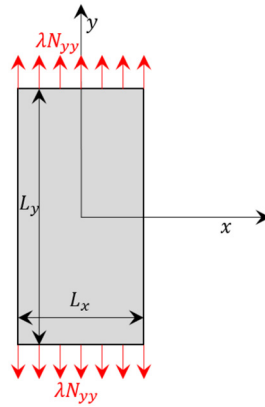


Fig. 1. Membrane under uniaxial traction.

Table 1

Number of inversions of the tangent matrix for different truncation orders with deformations K_1 and K_2 required by the ANM algorithm and by the Abaqus industrial code.

Truncation order p	10	15	20	25
Number of inversions for (K_1)	72	54	47	44
Number of inversions for (K_2)	60	44	39	36
Number of inversions for (Abaqus)	246 iterations			

where ε is a given tolerance parameter. Once a_{\max} is calculated, the starting solution to the next step is evaluated by $(u^j, \lambda^j, \{\theta^j\}, \{S^j\}) = (u(a_{\max}), \lambda(a_{\max}), \{\theta\}(a_{\max}), \{S\}(a_{\max}))$.

4. Wrinkling disappearance analysis

We shall first show numerically, by using the ANM presented in section 3, that when we neglect the order-2 terms of $u_{,x}$, $u_{,y}$, $v_{,x}$ and $v_{,y}$ in the expression of the nonlinear part of the deformation vector (3), as it is usual in the context of the FvK theory for buckling problems, the bifurcation curves do not coincide with those obtained by the Abaqus code. We shall show that we can find the bifurcation curves when we add these terms in the definition of the deformation, as indicated in the expression (3).

For this purpose, we study the wrinkles of a thin membrane under uniaxial loading λN_{yy} on the sides $y = L/2$ and $y = -L/2$ in the y direction; with $N_{yy} = 1$ N/mm and $u(0, y) = v(0, y) = 0$ and free on the other sides. The thin membrane, of width $L_x = 50$ mm, of length $L_y = 100$ mm and of thickness $h = 0.05$ mm, is made of an elastic, homogeneous and isotropic material of Young’s modulus $E = 70000$ MPa and Poisson’s ratio $\nu = 0.3$ (see Fig. 1).

Due to the symmetry of the problem, a quarter of the membrane is considered and discretized into DKT18 elements, i.e. 12870 ddl [20] for the ANM and into S8R elements, i.e. 9798 ddl, when we use the industrial Abaqus code. Here, the objective is to study numerically the instability of the membrane by using two types of deformations; that of the formula (9) and the one that does not take into account the squares of the terms $u_{,x}$, $v_{,x}$, $u_{,y}$ and $v_{,y}$ (10), which are denoted in the following by K_1 and K_2 , respectively.

In Table 1, we discuss the influence of the truncation order p on the number of steps in the ANM algorithm for a tolerance parameter $\varepsilon = 10^{-6}$. From this table, we remark that the step length increases with the truncation order. Based on this observation, we remark that the results require a smaller computation time for the order $p = 15$ than for high orders. We also notice that the number of inversions of the tangent matrix decreases as the truncation order increases.

In the following, the numerical control parameters of the ANM are: tolerance parameter $\varepsilon = 10^{-6}$, truncation order $p = 15$. In Fig. 2, we represent the load–displacement curves (λ, w) at the central node of the membrane obtained by the ANM algorithm with deformations K_1 and K_2 and by the industrial Abaqus code. In this figure, we note that the first bifurcation load obtained by the two algorithms is the same for the two deformations K_1 and K_2 . The disappearance of wrinkles is observed only for the deformation K_1 and that used by the industrial code Abaqus. For the deformations K_1 and K_2 , the load–displacement curve is obtained respectively in 54 and 46 steps of ANM algorithm (54 and 44 inversions of the tangent matrix). On the other hand, the load–displacement curve is obtained in 246 inversions of the tangent matrix when the Abaqus industrial code is used. From the obtained results, we see that when using the deformation K_1 , we can detect the phenomenon of wrinkle disappearance, but we can not observe this phenomenon when we use the deformations K_2 .

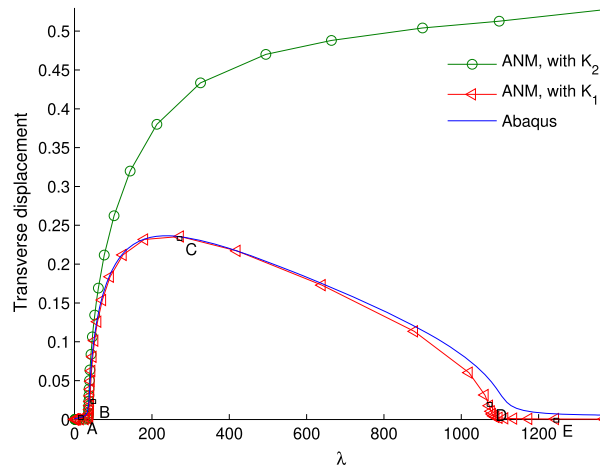


Fig. 2. Load–displacement curve (λ, w) at the central node of the membrane ($x = \frac{L_x}{2}, y = \frac{L_y}{2}$) obtained by the ANM with deformations K_1 and K_2 and by the industrial Abaqus code for $h = 0.05$ mm and $\beta = 2$.

This figure shows also the positions in which the deformation state of the membrane is visualized. For this, five positions are chosen; the two first ones are located before and after the first bifurcation point, the third position represents the maximum displacement value, and the last two positions are before and after the second bifurcation point.

In Fig. 3, we represent the deformations of the line $y = \frac{L_y}{2}$ and of the membrane for the positions A, B, C, D, and E represented in Fig. 2. It should be noted that, in the first position A, the transverse displacement w is always zero. Concerning position B, it is seen that there is appearance of wrinkles with a small amplitude. At position C, it is observed that there are wrinkles having a maximum amplitude. From position D onwards, the amplitude of the wrinkles decreases and disappears at position E.

4.1. Influence of the thickness h and of the aspect ratio β

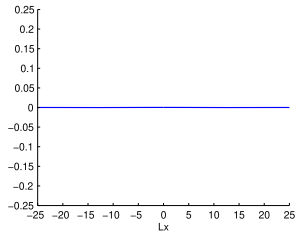
In the following, we are interested in studying the influence of the thickness h of the membrane on the load–displacement curves of bifurcation obtained by the ANM algorithm using only the deformation K_2 . For this purpose, the same numerical data as the previous ones is used. The considered values of h are: $h = 0.01$ mm, $h = 0.02$ mm, $h = 0.03$ mm, $h = 0.04$ mm, $h = 0.05$ mm, and $h = 0.06$ mm, $h = 0.07$ mm, $h = 0.08$ mm, $h = 0.09$ mm, $h = 0.100$ mm, $h = 0.103$ mm, and $h = 0.105$ mm. In Fig. 4, we represent the load–displacement curves at the central node obtained by the ANM algorithm for different values of the thickness h . From the obtained results, we notice that there are two different bifurcation points. The first bifurcation point corresponds to the appearance of the wrinkles and the second point corresponds to their disappearance. We have used a very fine mesh to ensure convergence of the solution, and we have compared the obtained results with those of Abaqus for the thickness values $h = 0.002$ mm and $h = 0.004$ mm. This behavior was not observed when we used the FvK theory, in which case an increase in the amplitude would have been obtained as h increased. According to these results, it can be seen that, when the thickness is increased, the amplitude of wrinkling increases up to a value $h = 0.05$ mm and, beyond this thickness, this amplitude decreases and ends with the disappearance of wrinkles. In this study, we remark also that wrinkling appear only on the interval $h \in [0.01; 0.106]$.

In the following, we are interested in studying the influence of the aspect ratio $\beta = \frac{L_y}{L_x}$ on the instability of the membrane as well as on the disappearance of wrinkles. For that, we adopt the same numerical control parameters of the ANM and the thickness $h = 0.05$ mm. For this study, we fix the width of the membrane L_x at 50 mm, and we adopt the numerical values of the aspect ratio $\beta = 1.4$, $\beta = 1.5$, $\beta = 1.6$, $\beta = 1.7$, $\beta = 1.8$, $\beta = 1.9$, $\beta = 2$, and $\beta = 2.5$.

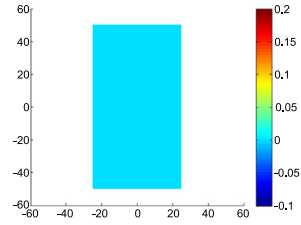
In Fig. 5, we represent the load–displacement curves at the central node obtained by the ANM algorithm for the different values of the aspect ratio β . According to these results, it is clearly seen that, when the value of the aspect ratio is strictly less than 1.4, the membrane remains in its plane and, from this value, it is noted that there is appearance and disappearance of wrinkling.

5. Conclusion

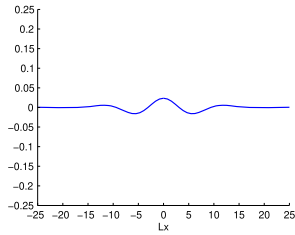
In this paper, we have investigated disappearance of wrinkles from a stretched membrane by the Asymptotic Numerical Method (ANM). We have adopted a deformation that depends on membrane displacements, which we have compared to the deformation of the Föppl–von Kármán model. We have observed that there is appearance and disappearance of wrinkling when we used the deformation for specific values of the thickness h and of the aspect ratio β . With the deformation of the Föppl–von Kármán model, we have numerically demonstrated that there is no disappearance of the wrinkling. The ANM



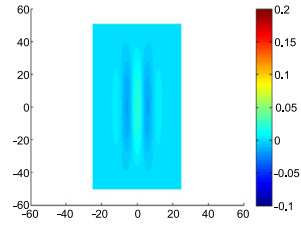
(a) Deformation of the line $y = \frac{L_y}{2}$ for position A.



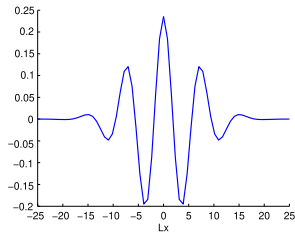
(b) Deformation of the membrane for position A.



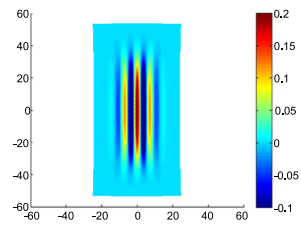
(c) Deformation of the line $y = \frac{L_y}{2}$ for position B.



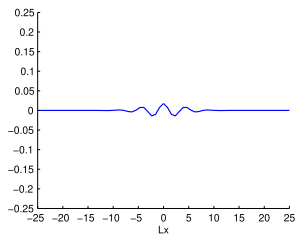
(d) Deformation of the membrane for position B.



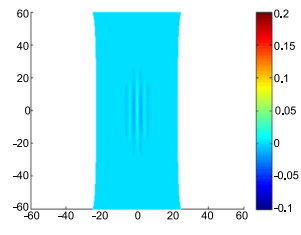
(e) Deformation of the line $y = \frac{L_y}{2}$ for position C.



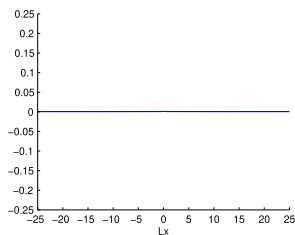
(f) Deformation of the membrane for position C.



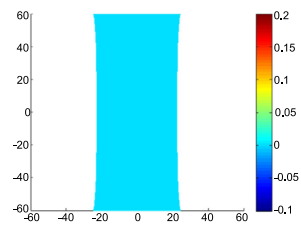
(g) Deformation of the line $y = \frac{L_y}{2}$ for position D.



(h) Deformation of the membrane for position D.



(i) Deformation of the line $y = \frac{L_y}{2}$ for position E.



(j) Deformation of the membrane for position E.

Fig. 3. Deformations of the line $y = \frac{L_y}{2}$ and of the membrane for different positions and for $h = 0.05$ mm and $\beta = 2$.

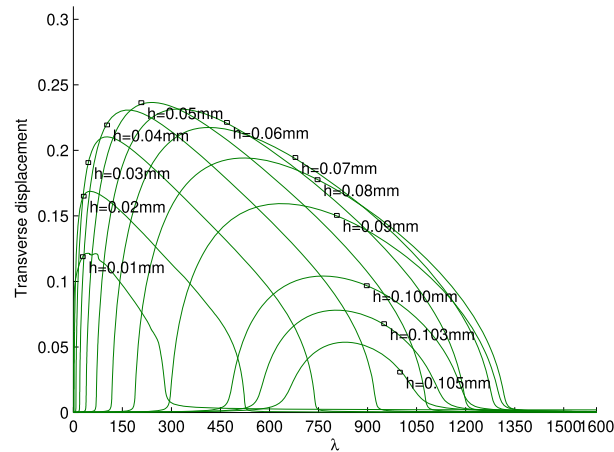


Fig. 4. Load–displacement curves of bifurcation at the central node of the membrane obtained by the ANM algorithm for different values of the thickness h .

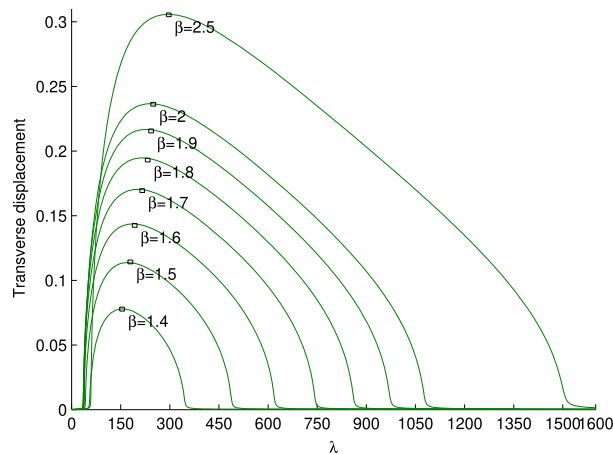


Fig. 5. Load–displacement curves of bifurcation at the central node of the membrane obtained by ANM for different values of the aspect ratio β .

algorithm coupled with the finite-element method is used for the first time for such problems. The use of this algorithm has greatly reduced the computational time compared to the Abaqus code, and made the continuation easier. Indeed, the solution was obtained using a single combination of the parameters of the ANM algorithm, the truncation order and the tolerance parameter, from the starting point. The obtained results are compared to those obtained by the Abaqus industrial code.

References

- [1] A. Diaby, A. Le Van, C. Wielgosz, Modélisation du plissage dans les structures membranaires, *Eur. J. Comput. Mech.* 15 (1–3) (2006) 143–154.
- [2] S. Abdelkhalek, P. Montmitonnet, N. Legrand, P. Buessler, Manifested flatness predictions in thin strip cold rolling, *Int. J. Mater. Forming* 1 (1) (2008) 339–342.
- [3] Z. Cai, Y. Fu, On the imperfection sensitivity of a coated elastic half-space, *Proc. R. Soc. A* 455 (1999) 3285–3309.
- [4] Z. Cai, Y. Fu, Exact and asymptotic stability analyses of a coated elastic half-space, *Int. J. Solids Struct.* 37 (22) (2000) 3101–3119.
- [5] X. Chen, J.W. Hutchinson, Herringbone buckling patterns of compressed thin films on compliant substrates, *J. Appl. Mech.* 71 (5) (2004) 597–603.
- [6] Z. Huang, W. Hong, Z. Suo, Nonlinear analyses of wrinkles in a film bonded to a compliant substrate, *J. Mech. Phys. Solids* 53 (9) (2005) 2101–2118.
- [7] R. Huang, Kinetic wrinkling of an elastic film on a viscoelastic substrate, *J. Mech. Phys. Solids* 53 (1) (2005) 63–89.
- [8] T.J. Healey, Q. Li, R.-B. Cheng, Wrinkling behavior of highly stretched rectangular elastic films via parametric global bifurcation, *J. Nonlinear Sci.* 23 (5) (2013) 777–805.
- [9] H.B. Keller, Lectures on numerical methods in bifurcation problems, *Appl. Math.* 217 (1987) 50.
- [10] N. Friedl, F.G. Rammerstorfer, F.D. Fischer, Buckling of stretched strips, *Comput. Struct.* 78 (1–3) (2000) 185–190.
- [11] Q. Li, T.J. Healey, Stability boundaries for wrinkling in highly stretched elastic sheets, *J. Mech. Phys. Solids* 97 (2016) 260–274.
- [12] E. Fehér, T.J. Healey, A.A. Sipos, The Mullins effect in the wrinkling behavior of highly stretched thin films, *J. Mech. Phys. Solids* 119 (2018) 417–427.
- [13] T. Wang, C. Fu, F. Xu, Y. Huo, M. Potier-Ferry, On the wrinkling and restabilization of highly stretched sheets, *Int. J. Eng. Sci.* 136 (2019) 1–16.
- [14] C. Fu, T. Wang, F. Xu, Y. Huo, M. Potier-Ferry, A modeling and resolution framework for wrinkling in hyperelastic sheets at finite membrane strain, *J. Mech. Phys. Solids* 124 (2019) 446–470.
- [15] B. Cochelin, N. Damil, M. Potier-Ferry, *Méthode asymptotique numérique*, Hermès Lavoisier, 2007.

- [16] H. Mottaqui, B. Braikat, N. Damil, Discussion about parameterization in the asymptotic numerical method: application to nonlinear elastic shells, *Comput. Methods Appl. Mech. Eng.* 199 (25–28) (2010) 1701–1709.
- [17] L. Azrar, B. Cochelin, N. Damil, M. Potier-Ferry, An asymptotic-numerical method to compute the postbuckling behaviour of elastic plates and shells, *Int. J. Numer. Methods Eng.* 36 (8) (1993) 1251–1277.
- [18] B. Cochelin, N. Damil, M. Potier-Ferry, Asymptotic-numerical methods and Padé approximants for non-linear elastic structures, *Int. J. Numer. Methods Eng.* 37 (7) (1994) 1187–1213.
- [19] P. Vannucci, B. Cochelin, N. Damil, M. Potier-Ferry, An asymptotic-numerical method to compute bifurcating branches, *Int. J. Numer. Methods Eng.* 41 (8) (1998) 1365–1389.
- [20] J.-L. Batoz, G. Dhatt, *Modélisation des structures par éléments finis : Solides élastiques*, Presses de l'Université Laval, Québec, Canada, 1990.
- [21] B. Cochelin, A path-following technique via an asymptotic-numerical method, *Comput. Struct.* 53 (5) (1994) 1181–1192.